

## Completed Local Ternary Count for Rotation Invariant Texture Classification

<sup>1</sup>Ch. Sudha Sree and <sup>2</sup>M.V.P. Chandra Sekhara Rao

<sup>1</sup>Department of Computer Science and Engineering,  
University College of Engineering and Technology, Acharya Nagarjuna University,  
Nagarjuna Nagar, Andhra Pradesh (AP), India

<sup>2</sup>RVR and JC College of Engineering, Guntur, Andhra Pradesh (AP), India

---

**Abstract:** Rotation invariant texture classification is an important issue in image analysis. For more than a decade Local Binary Pattern (LBP) variants have been proven to be successful methods in wide applications of rotation invariant texture classification. However, these invariant patterns are not absolutely rotation invariant and some of these are noise sensitive/insensitive. Till date, no ternary LBP variant is found as rotation invariant and noise insensitive. This study proposes a rotation invariant and noise insensitive texture descriptors called, Local Ternary Count (LTC) and Completed Local Ternary Count (CLTC). The two descriptors characterize the textures using local ternary gray scale difference by avoiding the micro-structure. The proposed CLTC is a set of three new operators defined for sign, magnitude and central pixel components. Experiments are conducted on three well known benchmark databases Outex, UIUC and CURET. The performance of the proposed method is analysed by comparing with the various existing LBP variants. It is observed that, CLTC exhibits significant improvement in classification accuracy and is more robust to noise when compared with LBP variants at different Signal-to-Noise Ratio (SNR) values.

**Key words:** Local binary pattern, local ternary pattern, completed local binary count, rotation invariant, texture classification

---

### INTRODUCTION

Texture classification plays a vital role in computer vision and image processing applications such as object recognition, image retrieval, remote sensing and medical image analysis. As the real world texture images have observable orientation variations, the rotation invariant texture classification has become an important issue in practice.

Many textural feature extraction methods are proposed for rotation invariant texture classification. These methods are categorized into three classes (Zhang and Tan, 2002), namely statistical, model based and structural. Statistical methods represent texture by the statistics of selected features. Haralick *et al.* (1973) have used the co-occurrence matrix to extract the texture features from texture images. Fuzzy aura matrix (Hammouche *et al.*, 2016) is used for extracting the texture features from gray level and color images based on aura set. It extracts the features by involving neighborhood of each pixel of the image. In model based methods, texture is a probability model or linear combination of a set of basic functions. Zhao and Pietikainen (2007) proposed Improved Gaussian Markov Random-Field (IGMRF)

method to extract texture features. This method uses the step by step least square method to extract GMRF features. Markov random fields (Cao *et al.*, 2010) features are used to identify the spatial relationship between the body parts. In structural methods, the texture is represented by a hierarchy of spatial arrangements (macro-texture) and with well-defined primitives (micro-texture). Xu *et al.* (2016) developed a multiple morphological component analysis to extract multiple texture features from remote sensing images. These features are used to classify remote sensing images. Lam and Li (1997) have determined an Improved Iterative Morphological Decomposition (IIMD) method for texture classification.

The LBP brings together both statistical and structural approaches to extract the texture features. Among all these LBP is simple and became one of the successful methods in wide applications of texture classification. Ojala *et al.* (2002) proposed a multi-resolution grayscale and rotation invariant texture feature extraction methods like conventional Local Binary Pattern (LBP), Local Binary Pattern with rotation invariant (LBP<sup>r</sup>), LBP rotation invariant and uniform (LBP<sup>mi2</sup>), variance (VAR) and LBP<sup>mi2</sup>/VAR, LBP<sup>mi2</sup>/VAR has

---

**Corresponding Author:** Ch. Sudha Sree, Department of Computer Science and Engineering,  
University College of Engineering and Technology, Acharya Nagarjuna University, Nagarjuna Nagar,  
Andhra Pradesh, India

achieved the best classification accuracy when compared to others. LBP was used in many applications such as dynamic texture recognition (Zhao and Pietikainen, 2007), medical image analysis (Nanni *et al.*, 2010), face detection (Ouamane *et al.*, 2016), gender classification (Hadid *et al.*, 2015) and face recognition (Ahonen *et al.*, 2006). It is sensitive to noise and rotation invariant. Some of the work related to LBP, invariant to rotation is explained in the following lines. A noise insensitive, Dominant Local Binary Pattern (DLBP) (Liao *et al.*, 2009) is developed by Liao *et al.* The DLBP features represent the most frequently occurred patterns for texture images. It is observed that the DLBP method has maximum classification accuracy when compared to existing methodologies. Khellah (2011) introduced a texture descriptor method, Dominant Neighborhood Structure (DNS) to extract global features of image. It is robust to noise. It has achieved good classification accuracy when compared to LBP, dominant LBP and completed LBP. Further it is combined with LBP, achieved 99% of classification accuracy. A rotation invariant sorted consecutive Local Binary Pattern (scLBP) (Ryu *et al.*, 2015) is used to extract the patterns regardless of number of transitions. Guo *et al.* (2010) introduced a texture descriptor, LBP variance with global matching for rotation invariant texture classification. Median Binary Pattern (MBP) (Hafiane *et al.*, 2015) is proposed for texture classification similar to LBP. It is used the median value as the threshold instead of central pixel in thresholding process. A noise insensitive Adaptive Median Binary Pattern (AMBP) (Hafiane *et al.*, 2015) is used as a texture descriptor for texture classification. It computes the patterns based on adaptive analysis window and improves discriminative properties. Adjacent Evaluation Completed Local Binary Pattern (AECLBP) (Song *et al.*, 2015) is used to extract texture features. It is robust to noise by changing the threshold scheme of LBP with adjacent evaluation window. Completed Robust Local Binary Pattern (CRLBP) is defined by Zhao *et al.* (2013) for texture classification. Unlike LBP, the method has used a weighted local gray level for comparing neighboring pixel. It consists of three operators Robust Local Binary Pattern (RLBP), RLBP-Magnitude (RLBP-M) and RLBP-Center (RLBP-C). It is insensitive to noise with good classification accuracy. Shrivastava and Tyagi (2014) determined Completed Local Structure Pattern (CLSP) and Robust Local Structure Pattern (RLSP) for image texture classification. CLSP has three operators, namely Local Structural Pattern (LSP), Local Binary Pattern (LBP) and Central Pixel (CP) pattern. These three operators are combined using 3D joint histogram. It is sensitive to noise. RLSP is built by combining the three operators LSP, Robust Local Binary Pattern (RLBP) and CP. It is robust to noise. Dan *et al.* (2014) proposed an improved robust texture descriptor, the Joint Local Binary

Pattern with Weber-like responses (JLBPW) for texture classification. The JLBPW determines the local intensity differences based on Weber's law to make robust to noise. Tan and Triggs (2010) have proposed Local Ternary Pattern (LTP) which is an extension to LBP. It is noise insensitive. Guo *et al.* (2010) proposed the Completed Local Binary Pattern (CLBP) by combining conventional LBP with the measures of local gray scale difference, magnitude and central gray level. Zhao *et al.* (2012) have proposed a Completed Local Binary Count (CLBC). Unlike LBP, CLBC counts the number of one's of binary pattern after thresholding and thus became rotation invariant. The summarization of strengths of various LBP variant methods, so far is reported in Table 1. Though these methods are proposed as invariant but these are not absolutely invariant in practice except CLBC and scLBP. The demonstration is shown in Fig. 1. As a solution this study proposes a two rotation invariant and noise insensitive texture descriptors, Local Ternary Count (LTC) and Completed Local Ternary Count (CLTC).

#### **Rationale for the new proposed rotation invariance method:**

From the literature, so far the rotation invariance and noise insensitive/sensitive LBP variants are very few. These also may vary after rotation and interpolation. For example,  $LBP^n$  and Median Binary Pattern (MBP) are rotation invariants as shown in Table 1. But these patterns may vary after rotation and interpolation as demonstrated in the following figures from Fig. 1a, b. Since, the methods CLBP, JLBP, DLBP, AMBP, LTP, AECLBP, RLSP, CRLBP and CLSP follow the same rotation invariant process as in  $LBP^n$ , these are also not absolutely invariant patterns.  $LBP^n$  forms the  $LBP^{n \times 2}$ . So, it suffers with rotation variance. These observations show that all the noise insensitive LBP rotation invariant patterns may vary after rotation and interpolation. This disadvantage can be overcome by counting the number of one's in the binary code instead of encoding. So, we propose rotation invariant and noise insensitive texture descriptors Local Ternary Count (LTC) and Completed Local Ternary Count (CLTC).

#### **The contributions:**

- Two rotation invariant and noise insensitive local texture descriptors LTC and CLTC are proposed
- CLTC has been defined with a set of three operators
- The two new descriptors are proposed to represent macrostructure
- More discriminating capability is assigned through ternary pattern
- Significant improvement is observed with noise over all the existing methods in terms of classification accuracy

Table 1: Strengths of various LBP variants

Years	LBP variant	Rotation		Noise		Texture features	
		Variant	Invariant	Sensitive	Insensitive	Local	Global
2002	Conventional LBP	✓		✓		✓	✓
2002	LBP <sup>n1</sup>	✓		✓	✓		
2002	LBP <sup>n2</sup>	✓		✓	✓		✓
2002	VAR		✓			✓	
2009	DLBP		✓		✓	✓	
2011	DNS+LBP		✓				✓
2015	MBP		✓			✓	
2015	scLBP		✓			✓	
2010	LBPV		✓				
2010	LBPV+Global matching		✓				✓
2015	AMBP		✓		✓	✓	
2010	CLBP		✓		✓	✓	
2013	CRLBP		✓		✓	✓	
2014	CLSP		✓	✓		✓	
2014	RLSP		✓		✓	✓	
2014	JLBP		✓			✓	
2010	LTP		✓		✓	✓	
2015	AECLBP		✓		✓	✓	
2012	CLBC		✓				

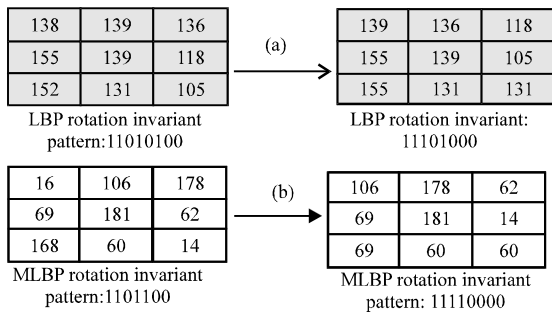


Fig. 1: Rotation invariant patterns may vary after rotation: a) LBP<sup>n</sup> and b) MBP

MATERIALS AND METHODS

**Local ternary count and completed local ternary count:** From literature review, noise insensitive LBP variants suffered from rotation variant. We have proposed a new rotation invariant and noise insensitive texture descriptor namely LTC and CLTC. It provides the discrete patterns using threshold t.

**Local Ternary Count (LTC):** We have defined the LTC with a ternary code as opposed to LBP which contains a binary pattern. It is experimentally proved that in LTP the ternary code improves noise insensitivity. Unlike LTP we have framed LTC without encoding step to make rotation invariant. It is described in detail as follows: In LTC, each pixel in the local neighbor set turned to one of the ternary values (-1, 0, 1) after comparison with its central pixel. This ternary pattern is divided into two patterns. One pattern is lower and other is upper. The lower pattern is built by placing 1 at -1 and remaining zeros and upper pattern is built by placing 1 at 1 and remaining zeros. It counts the

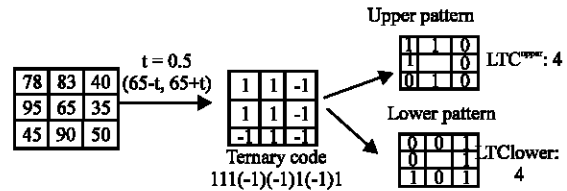


Fig. 2: LTC operator

frequency of ones in lower and upper patterns as shown in Fig. 2. Then, histograms are built for each and concatenated into one histogram. LTC is defined as follows:

$$LTC_{P,R} = \sum_{p=0}^{P-1} S(g_p - g_c), \quad (1)$$

$$S(x) = \begin{cases} 1, & x \geq t \\ 0, & -t < x < t \\ -1, & x \leq -t \end{cases}$$

LTC<sup>upper</sup><sub>P,R</sub> is defined as:

$$LTC_{P,R}^{upper} = \sum_{p=0}^{P-1} S(g_p - (g_c + t)), \quad (2)$$

$$S(x) = \begin{cases} 1, & x \geq 0 \\ 0, & \text{otherwise} \end{cases}$$

LTC<sup>lower</sup><sub>P,R</sub> is defined as:

$$LTC_{P,R}^{lower} = \sum_{p=0}^{P-1} S(g_p - (g_c - t)), \quad (3)$$

$$S(x) = \begin{cases} 1, & x \leq 0 \\ 0, & \text{otherwise} \end{cases}$$

Where:

- $g_c$  = Gray value of central pixel
- $g_p$  ( $p = 0, \dots, P-1$ ) = Gray value of neighboring pixel on a circle of radius
- $R, P$  = The number of neighborhood pixels
- $t$  = Threshold

It is defined by user. Further, we have enhanced LTC to Completed Local Ternary Count (CLTC) to improve performance of texture classification.

**Completed Local Ternary Count (CLTC):** It extracts the completed local texture information. It contains CLTC\_Sign (CLTC\_S), CLTC\_Magnitude (CLTC\_M) and CLTC\_Center (CLTC\_C). CLTC\_S is same as LTC. CLTC<sub>MP,R</sub> is built with concatenation of the histograms of CLTC<sub>MP,R</sub><sup>upper</sup> and CLTC<sub>MP,R</sub><sup>lower</sup>. CLTC<sub>MP,R</sub><sup>upper</sup> is defined as follows:

$$CLTC_{MP,R}^{upper} = \sum_{p=0}^{P-1} M(|g_p - (g_c + t)|), \quad (4)$$

$$M(x) = \begin{cases} 1, & x \geq au \\ 0, & \text{otherwise} \end{cases}$$

where,  $au$  is average of  $|g_p - (g_c + t)|$  of whole image. CLTC<sub>MP,R</sub><sup>lower</sup> is defined as:

$$CLTC_{MP,R}^{lower} = \sum_{p=0}^{P-1} M(|g_p - (g_c - t)|), \quad (5)$$

$$M(x) = \begin{cases} 1, & x \geq al \\ 0, & \text{otherwise} \end{cases}$$

where,  $al$  is average of  $|g_p - (g_c - t)|$  of whole image.  $g_c, g_p, P, R$  and  $t$  are described as in Eq. 1. CLRC-C is constructed with the histograms of CLTC<sub>CP,R</sub><sup>upper</sup> and CLTC<sub>CP,R</sub><sup>lower</sup>. CLTC<sub>CP,R</sub><sup>upper</sup> is defined as:

$$CLTC_{CP,R}^{upper} = C(g_c + t), \quad (6)$$

$$C(x) = \begin{cases} 1, & x \geq c_1 \\ 0, & \text{otherwise} \end{cases}$$

CLTC<sub>CP,R</sub><sup>lower</sup> is defined as follows:

$$CLTC_{CP,R}^{lower} = C(g_c - t), \quad (7)$$

$$C(x) = \begin{cases} 1, & x \geq c_1 \\ 0, & \text{otherwise} \end{cases}$$

where,  $c_1$  is mean gray values of whole image.  $g_c, P, R$  and  $t$  are described as in Eq. 1. The final operator

CLTC histogram is built by merging the proposed CLTC operators into hybrid or joint distributions.

## RESULTS AND DISCUSSION

The experiments are conducted to evaluate the efficiency of CLTC with and without noise. The performance of CLTC in the presence of noise is studied by adding Gaussian noise with different Signal-to-Noise Ratio (SNR = 60, 50, 40 and 30 dB) values to the input images. The noise in the texture is increased while decreasing the SNR value. The performance of the proposed Completed Local Ternary Count (CLTC) is evaluated by conducting experiments on 11 different case studies from three huge databases. The results of proposed CLTC are compared with existing LBP variants results. The details of bench mark databases and various case studies are provided as follows:

**Outex database and case studies:** Outex database (Ojala *et al.*, 2002) contains Outex-TC-0010 (TC10) and Outex-TC-0012 (TC12) test suit. The TC10 and TC12 have 24 classes of texture images. These were collected under three illuminations (horizon, inca and t184) and nine various rotation angles (0°, 5°, 10°, 15°, 30°, 45°, 60°, 75° and 90°). Each class has 20 non overlapping 128\*128 texture images under each situation. The Outex database images are distributed into three different sets of case studies. Each set contains a set of trained and test data images. Experiments are conducted on each case study and the detailed description is as follow:

**Case study 1:** The 480 images of TC10 are used as training data. These are the images of each class under inca illumination with 0° rotation of angle. The 3840 images are used for testing. These are images of each class under same illumination with remaining rotation of angles (5°, 10°, 15°, 30°, 45°, 60°, 75° and 90°).

**Case study 2:** The images of TC12 with 0° rotation angle and inca illumination are taken for training and images of TC12 under illumination t184 has taken as for testing.

**Case study 3:** The images of TC12 with inca illumination and 0° rotation angle are taken as trained data and the images of TC12 under the illumination horizon are considered as test data.

**Columbia-Utrecht Reflection and Texture (CURET) Database and case studies:** The CURET database (Dana *et al.*, 1999) has 61 classes of textures captured at various viewpoints and illumination orientations. Each class has 92 images. N images for each class are randomly

selected as train data and remaining (92-N) images for each class are selected as test data for classification where N = 6, 12, 23 and 46. The case studies of CURET database are as follows:

**Case study 1:** From each class 6 images are randomly selected as train data and remaining images of each class are taken as test data.

**Case study 2:** The 12 images from each class are randomly selected for train data and the remaining (92-12) images of each class as test data.

**Case study 3:** The 23 images of each class are randomly selected for training and testing is conducted on remaining images.

**Case study 4:** From each class 46 images are randomly selected for training and the remaining images of each class are taken for testing.

**UIUC database and case studies:** UIUC database (Lazebnik *et al.*, 2005) contains 25 classes. Each class has 40 images with resolution of 640×480. These images are retrieved under significant viewpoint variations. N images of each class are randomly selected as train data and remaining (40-N) images of each class are selected as test data for classification. The details of UIUC database are as follows.

**Case study 1:** From each class, 5 images are randomly selected as train data and remaining images of each class are taken as test data.

**Case study 2:** The 10 images from each class are randomly selected for training and the left out images of each class are taken as test data.

**Case study 3:** The 15 images are randomly selected from each class for training and the remaining images of each class considered for testing.

**Case study 4:** From each class, 20 images are randomly selected for training and the left out images of each class are taken as test data. Different classification accuracy values are observed in different independent executions of the methods with noise. The range of variability and average classification accuracy is noted by running each method including the proposed method 20 times on each case study. Classification accuracy is measured based on the dissimilarity of distance between two histograms. Chi-square statistics is used for measuring dissimilarity of the two histograms. The formula is as follows:

$$\text{Dissimilarity}_{\chi^2}(H, K) = \sum_{i=1}^B \frac{(h_i - k_i)^2}{h_i + k_i} \quad (8)$$

where, H =  $h_i$  and K =  $k_i$  where (i = 1, 2, 3, ..., B) represents histograms. The nearest neighborhood classifier is used for classification. The classification performance is measured using following equation:

$$\text{Classification performance} = \frac{N_{\text{right}}}{M} \times 100 \quad (9)$$

Where:

$N_{\text{right}}$  = The number of right classifications

M = Number of images in test data

Experiments are conducted with radius R = 1, 2 and 3, neighboring pixels P = 8, 16 and 24, threshold t = 0.5. The experiments are conducted on Intel (R) Core (TM) 2.4 GHz, 8GB RAM, Windows 10 Operating System machine using MATLAB 2008b. The results from the experiments on TC10, TC12 (t184), TC12 (horizon) without noise are presented in Table 2. The experimental results for N = 6, 12, 23, 46 on CURET database without noise is shown in Table 3. The experimental results on UIUC without noise when N = 5, 10, 15 and 20 are tabulated in the Table 4. The results from the experiments on TC10, TC12 (t184) with noise are tabulated in Table 5 and 6. The experimental results for N = 6 and 46 of CURET with noise are presented in Table 7 and 8. The experimental results of UIUC for N = 5 and 20 with noise are shown in Table 9 and 10.

Experiments are aimed to evaluate the performance of CLTC with and without noise. When the experiments are conducted with noise, the results of CLTC compared with LBP<sup>nu2</sup>, CLBP, CLBC and LTP. Whereas the experiments conducted without noise the CLTC performance is evaluated based on efficiency of LTP, LBP<sup>nu2</sup>, LBP<sup>n</sup>, VAR, LBP<sup>nu2</sup>/VAR, CLBP and CLBC. Brief discussions on these results are as follows:

**Without noise:** From Table 2, it is found that the proposed CLTC\_S\_M\_C has achieved average classification accuracies 93.31, 95.76, 95.76% at radius R = 1, 2 and 3 on Outex. From the Table 3, it is observed that, it has achieved mean classification accuracies 86.16, 87.41, 86.72 for radius R = 1, 2 and 3 on CURET. Table 4 demonstrated that, CLTC\_S\_M\_C achieved average classification accuracies in order 84.65, 87.29, 87.45% on UIUC. We observed that, it performed better when compared to LTP, LBP<sup>nu2</sup>, LBP<sup>n</sup>, VAR and LBP<sup>nu2</sup>/VAR. When compared to CLBP\_S\_M\_C, the CLTC\_S\_M\_C is rotation invariant and performed equally well, even though it avoids the representation of

Table 2: Classification accuracy (%) on TC10 and TC12 of various LBP variants

Variables	R = 1, P = 8				R = 2, P = 16				R = 3, P = 24					
	TC10	TC12	t184	Horizon	Average	TC10	t184	TC12	Horizon	Average	TC10	t184	TC12	Horizon
LTP	94.14	75.88	73.96	81.33	81.33	96.95	90.16	86.94	91.35	98.20	93.59	89.42	93.74	
LBP <sup>min2</sup>	84.81	65.46	63.68	71.32	71.32	89.40	82.27	75.21	82.29	95.08	85.05	80.79	86.97	
LBP <sup>n</sup>	78.80	71.97	69.98	73.58	73.58	91.72	88.26	88.47	89.48	-	-	-	-	
VAR	88.39	61.48	62.34	70.74	70.74	86.61	63.26	68.94	72.94	-	-	-	-	
LBP <sup>min2</sup> /VAR	95.63	75.93	74.91	82.16	82.16	97.08	84.40	83.19	88.22	-	-	-	-	
CLBP_S	84.81	65.46	63.68	71.32	71.32	89.40	82.26	75.21	82.29	95.07	85.04	80.78	86.96	
CLBC_S	82.94	65.02	63.17	70.38	70.38	88.67	82.57	77.41	82.88	91.35	83.82	82.75	85.97	
CLTC_S	87.79	73.99	73.77	78.52	78.52	91.25	86.96	82.22	86.81	92.19	86.11	85.21	87.84	
CLBP_M	81.74	59.30	62.77	67.94	67.94	93.67	73.79	72.40	79.95	95.52	81.18	78.65	85.12	
CLBC_M	78.96	53.63	58.01	63.53	63.53	92.45	70.35	72.64	78.48	91.85	72.59	74.58	79.67	
CLTC_M	92.19	73.94	69.95	78.69	78.69	96.38	83.84	83.54	87.92	96.41	85.10	86.02	89.18	
CLBP_S_M	94.66	82.75	83.14	86.85	86.85	97.89	90.55	91.11	93.18	99.32	93.58	93.35	95.42	
CLBC_S_M	95.23	82.12	83.59	86.98	86.98	98.10	89.95	90.42	92.82	98.70	91.41	90.25	93.45	
CLTC_S_M	96.22	83.43	83.91	87.85	87.85	97.94	89.93	89.88	92.58	98.80	90.67	89.40	92.96	
CLBP_S_M_C	96.56	90.30	92.29	93.05	93.05	98.72	93.54	93.91	95.39	98.93	95.32	94.53	96.26	
CLBC_S_M_C	97.16	89.79	92.92	93.29	93.29	98.54	93.26	94.07	95.29	98.78	94.00	93.24	95.34	
CLTC_S_M_C	97.29	89.91	92.73	93.31	93.31	98.88	94.03.00	94.38	95.76	98.98	94.54	93.75	95.76	

Table 3: Classification accuracy (%) on CUREt of various LBP variants

Variables	R = 1, P = 8				R = 2, P = 16				R = 3, P = 24			
	6	12	23	46	6	12	23	46	6	12	23	46
LTP	55.28	63.87	73.75	80.47	55.91	64.18	71.25	79.86	50.51	58.65	66.50	72.24
LBP <sup>min2</sup>	60.36	69.05	74.64	81.32	63.38	72.70	79.28	84.53	67.86	75.51	81.65	86.35
LBP <sup>n</sup>	66.60	75.10	80.47	86.06	68.34	75.27	80.61	85.21	-	-	-	-
VAR	43.27	49.63	55.55	61.72	41.16	45.31	50.61	55.95	-	-	-	-
LBP <sup>min2</sup> /VAR	71.56	80.90	86.96	92.91	73.20	81.60	88.19	94.23	-	-	-	-
CLBP_S	60.36	69.05	74.64	81.32	63.38	72.70	79.28	84.53	67.86	75.51	81.65	86.35
CLBC_S	58.81	66.76	72.61	77.76	60.24	67.79	73.63	79.00	61.95	68.05	73.79	77.69
CLTC_S	61.38	71.37	77.95	86.03	64.85	74.75	80.49	89.77	66.93	74.67	79.78	89.84
CLBP_M	54.19	60.77	67.21	75.73	59.60	68.25	76.52	81.32	64.86	71.43	80.42	87.31
CLBC_M	45.06	50.98	56.33	64.33	50.27	59.49	65.91	71.53	52.23	59.26	69.11	75.20
CLTC_M	65.54	74.71	81.04	85.89	68.99	77.00	84.01	90.02	68.36	76.00	85.06	89.52
CLBP_S_M	74.41	82.9	88.9	92.62	76.47	84.32	89.92	93.30	77.90	84.73	90.99	93.97
CLBC_S_M	72.17	80.82	87.00	91.59	73.79	81.78	89.36	93.30	72.84	80.76	88.29	93.01
CLTC_S_M	72.91	81.05	87.74	93.26	74.78	82.66	89.76	95.01	73.37	81.25	89.50	94.73
CLBP_S_M_C	76.82	84.96	91.54	95.33	78.07	86.45	92.30	95.40	78.99	86.37	92.51	95.90
CLBC_S_M_C	75.09	83.32	90.66	94.23	76.65	84.12	92.42	95.15	76.00	83.38	91.35	95.01
CLTC_S_M_C	75.09	84.08	91.14	94.33	76.71	84.36	92.73	95.83	76.00	84.04	91.33	95.51

Table 4: Classification accuracy (%) on UIUC of various LBP variants

Variables	R = 1, P = 8				R = 2, P = 16				R = 3, P = 24			
	5	10	15	20	5	10	15	20	5	10	15	20
LTP	50.06	58.27	64.64	67.80	61.26	71.33	74.40	78.20	60.91	74.53	78.72	83.40
LBP <sup>min2</sup>	41.02	49.20	52.16	56.40	41.25	52.00	58.08	57.20	45.25	56.26	59.84	64.60
LBP <sup>n</sup>	43.89	50.80	57.12	63.20	49.26	60.67	66.56	71.80	-	-	-	-
VAR	36.34	43.73	47.84	49.80	39.20	47.33	50.40	51.00	-	-	-	-
LBP <sup>min2</sup> /VAR	51.77	63.07	67.84	67.80	58.86	67.33	71.04	73.80	-	-	-	-
CLBP_S	41.02	49.20	52.16	56.40	41.25	52.00	58.08	57.20	45.25	56.26	59.84	64.60
CLBC_S	40.00	48.80	51.36	56.80	42.17	54.27	58.56	62.00	48.34	59.87	62.72	67.80
CLTC_S	43.77	50.67	55.36	59.20	49.71	58.93	64.00	68.20	52.69	66.13	68.64	74.40
CLBP_M	40.45	52.26	55.84	57.40	58.17	66.00	69.92	72.40	58.40	67.33	71.52	76.40
CLBC_M	40.57	46.26	49.60	53.40	51.09	60.00	65.92	69.80	54.17	61.07	67.84	70.00
CLTC_M	50.06	61.07	66.88	71.00	60.23	71.47	73.60	80.00	63.66	74.00	75.20	82.40
CLBP_S_M	66.05	75.86	80.48	83.80	73.14	82.00	85.76	88.60	75.08	84.26	86.40	90.00
CLBC_S_M	66.17	75.47	80.00	82.80	76.11	82.67	86.24	89.80	76.46	86.67	87.36	89.80
CLTC_S_M	68.11	76.27	80.64	84.80	76.46	84.40	86.24	90.40	77.03	86.67	87.52	89.80
CLBP_S_M_C	75.20	84.93	86.08	88.20	81.26	86.40	89.12	92.20	79.65	87.06	87.52	93.00
CLBC_S_M_C	75.43	85.47	86.88	88.60	80.69	87.20	88.16	92.60	81.02	86.80	89.28	92.40
CLTC_S_M_C	76.69	85.60	87.52	88.80	80.91	87.33	88.32	92.60	81.37	86.80	89.44	92.20

Table 5: The classification accuracy (%) and range of variability in classification of accuracy on TC10

Variables	Accuracy with noise											
	R = 1				R = 2				R = 3			
	SNR = 60	SNR = 50	SNR = 40	SNR = 30	SNR = 60	SNR = 50	SNR = 40	SNR = 30	SNR = 60	SNR = 50	SNR = 40	SNR = 30
LBP <sup>ns2</sup>	36.79±0.21	36.07±0.23	31.31±0.30	13.84±0.25	87.59±0.14	87.00±0.36	84.44±0.40	42.38±0.22	94.14±0.13	94.11±0.18	92.75±0.25	58.27±0.38
CLBP <sub>-</sub>												
M_C	92.81±0.1	92.47±0.26	91.05±0.12	32.37±0.21	98.48±0.09	98.45±0.12	98.15±0.13	65.03±0.36	98.96±0.05	99.00±0.09	98.83±0.13	80.68±0.26
CLBC <sub>-</sub>												
S_M_C	92.10±0.25	91.78±0.22	90.89±0.10	36.76±0.14	97.77±0.17	97.77±0.20	96.85±0.16	87.25±0.27	98.65±0.1	98.62±0.13	98.49±0.13	96.42±0.14
CLTC <sub>-</sub>												
S_M_C	97.44±0.07	96.74±0.17	94.96±0.16	39.77±0.18	98.88±0.10	98.86±0.09	97.78±0.16	89.82±0.31	98.99±0.08	99.01±0.09	98.91±0.10	97.22±0.22
LTP	92.55±0.1	92.16±0.1	89.0±0.30	21.50±0.25	96.88±0.05	96.88±0.13	96.08±0.14	54.26±0.17	98.16±0.09	98.15±0.08	97.45±0.16	66.29±0.20

Table 6: The classification accuracy (%) and range of variability in classification of accuracy on TC12 (t184)

Variables	Accuracy with noise											
	R = 1				R = 2				R = 3			
	SNR = 60	SNR = 50	SNR = 40	SNR = 30	SNR = 60	SNR = 50	SNR = 40	SNR = 30	SNR = 60	SNR = 50	SNR = 40	SNR = 30
LBP <sup>ns2</sup>	39.03±0.19	38.83±0.13	32.85±0.28	14.39±0.15	80.44±0.37	80.10±0.24	76.62±0.39	37.88±0.36	84.5±0.24	84.32±0.34	82.03±0.24	55.78±0.22
CLBP <sub>-</sub>												
S_M_C	83.99±0.15	83.89±0.23	81.12±0.20	28.46±0.24	93.25±0.15	93.30±0.17	92.88±0.15	52.66±0.25	95.07±0.09	95.05±0.13	94.92±0.19	70.50±0.41
CLBC <sub>-</sub>												
S_M_C	82.95±0.10	82.53±0.15	80.59±0.27	31.89±0.28	92.70±0.09	92.80±0.16	91.98±0.15	75.71±0.27	93.77±0.21	93.73±0.09	93.52±0.28	87.56±0.31
CLTC <sub>-</sub>												
S_M_C	89.72±0.10	90.12±0.14	85.93±0.25	35.38±0.20	94.10±0.09	94.11±0.13	92.85±0.16	76.26±0.42	93.72±0.08	93.47±0.14	94.43±0.09	88.48±0.24
LTP	77.57±0.19	77.59±0.32	68.11±0.45	17.64±0.19	90.80±0.10	90.67±0.12	86.77±0.17	48.99±0.31	93.94±0.14	93.81±0.08	92.49±0.17	60.57±0.36

Table 7: The classification accuracy and range of variability in classification of accuracy on CURET (N = 6)

Variables	Accuracy with noise											
	R = 1				R = 2				R = 3			
	SNR = 60	SNR = 50	SNR = 40	SNR = 30	SNR = 60	SNR = 50	SNR = 40	SNR = 30	SNR = 60	SNR = 50	SNR = 40	SNR = 30
LBP <sup>ns2</sup>	31.68±0.15	31.77±0.16	31.87±0.25	26.58±0.30	56.53±0.28	56.29±0.23	55.87±.29	48.58±0.31	66.09±0.29	65.74±0.20	65.11±0.26	56.73±0.21
CLBP <sub>-</sub>												
S_M_C	71.16±0.06	70.88±0.10	70.40±0.13	60.97±0.31	77.49±0.10	77.32±0.25	76.82±0.11	70.39±0.29	78.75±0.10	78.87±0.16	78.09±0.16	72.54±0.24
CLBC <sub>-</sub>												
S_M_C	69.72±0.12	69.79±0.17	69.03±0.16	61.45±0.16	76.02±0.13	76.16±0.14	75.60±0.21	71.51±0.28	75.72±0.07	75.54±0.15	75.10±0.20	72.41±0.24
CLTC <sub>-</sub>												
S_M_C	75.11±0.07	73.60±0.14	71.36±0.13	61.48±0.15	76.92±0.10	76.67±0.06	76.13±0.09	71.77±0.15	75.97±0.08	75.91±0.11	75.33±0.11	72.55±0.11
LTP	65.06±0.10	65.09±0.12	63.50±0.15	52.42±0.23	68.70±0.13	68.96±0.08	68.27±0.07	61.18±0.18	73±0.1	72.95±0.11	72.56±0.18	65.79±0.28

Table 8: The classification accuracy and range of variability in classification of accuracy on CURET (N = 46)

Variables	Accuracy with noise											
	R = 1				R = 2				R = 3			
	SNR = 60	SNR = 50	SNR = 40	SNR = 30	SNR = 60	SNR = 50	SNR = 40	SNR = 30	SNR = 60	SNR = 50	SNR = 40	SNR = 30
LBP <sup>ns2</sup>	32.77±0.27	32.82±0.50	32.18±0.53	25.36±0.30	73.59±0.29	73.40±0.55	72.27±0.29	60.81±0.48	82.63±0.23	82.82±0.43	81.75±0.57	71.10±0.43
CLBP <sub>-</sub>												
S_M_C	85.82±0.14	85.31±0.18	84.52±0.20	73.75±0.23	94.74±0.16	94.55±0.25	94.03±0.23	85.80±0.20	95.88±0.20	96±0.23	95.38±0.20	88.85±0.25
CLBC <sub>-</sub>												
SMC	84.98±0.12	84.57±0.21	83.71±0.18	74.29±0.23	94.55±0.14	94.65±0.21	94.35±0.16	90.00±0.30	94.83±0.14	95.01±0.18	94.57±0.27	91.68±0.37
CLTC <sub>-</sub>												
SMC	94.33±0.11	92.00±0.16	89.16±0.16	75.46±0.23	95.63±0.14	95.19±0.12	95.09±0.14	90.94±0.12	95.50±0.06	95.32±0.11	94.91±0.14	91.99±0.11
LTP	87.83±0.2	86.96±0.21	83.59±0.30	67.50±0.39	91.39±0.12	91.20±0.18	90.24±0.18	80.65±0.29	91.73±0.25	91.75±0.30	91.18±0.23	83.18±0.32

microstructure information. It shows the superiority in classification accuracy when compared to CLBC\_S\_M\_C.

**With noise:** From Table 5 and 6, it is observed that, the proposed method CLTC\_S\_M\_C is more robust to noise when compared to LBP and LTP at different SNR

values. In average CLTC\_S\_M\_C is insensitive to noise when compared to CLBP\_S\_M\_C and CLBC\_S\_M\_C. It has achieved 39.77, 89.82 and 97.22 at radius 1, 2 and 3 when SNR is 30 dB on TC10. Similar observations are obtained by conducting the experiments on TC12 (horizon). Table 7 and 8 demonstrates that, CLTC\_S\_M\_C

**Table 9: The classification accuracy and range of variability in classification of accuracy on UIUC (N = 5)**

Variables	Accuracy with noise											
	R = 1				R = 2				R = 3			
	SNR = 60	SNR = 50	SNR = 40	SNR = 30	SNR = 60	SNR = 50	SNR = 40	SNR = 30	SNR = 60	SNR = 50	SNR = 40	SNR = 30
LBP <sup>32</sup>	21.31±0.17	21.09±0.17	23.14±0.14	18.4±0.34	38.4±0.34	38.46±0.29	37.71±0.46	31.14±0.4	44.69±0.23	44.46±0.23	45.37±0.23	36.69±0.46
CLBP												
S_M_C	75.03±0.06	75.09±0.11	71.77±0.22	46.91±0.17	81.2±0.17	81.09±0.17	80.4±0.17	65.37±0.46	79.6±0.06	80.06±0.06	78.91±0.17	68.17±0.29
CLBC												
S_M_C	74.86±0.11	75.2±0.11	72.63±0.17	51.03±0.04	80.86±0.06	80.63±0.17	79.83±0.17	71.26±0.29	81.43±0.06	81.43±0.06	81.09±0.17	75.03±0.29
CLTC												
S_M_C	76.41±0.14	76.61±0.09	74.06±0.12	51.04±0.11	80.8±0	80.7±0.06	79.22±0.23	71.85±0.29	81.44±0.06	81.57±0.17	80.99±0.17	75.73±0.11
LTP	50.05±0.05	49.77±0.06	49.26±0.23	29.6±0.23	60.74±0.17	60.29±0.29	61.09±0.29	49.43±0.29	61.03±0.11	60.69±0.23	61.37±0.11	54.74±0.23

**Table 10: The classification accuracy and range of variability in classification of accuracy on UIUC (N = 20)**

Variables	Accuracy with noise											
	R = 1				R = 2				R = 3			
	SNR = 60	SNR = 50	SNR = 40	SNR = 30	SNR = 60	SNR = 50	SNR = 40	SNR = 30	SNR = 60	SNR = 50	SNR = 40	SNR = 30
LBP <sup>32</sup>	26.5±0.3	25.9±0.3	26.2±0.6	22.8±0.4	55.5±0.5	55.6±0.4	55±0.8	38±0.6	63.9±0.3	64.1±0.5	45.8±0.6	63.3±0.5
CLBP												
S_M_C	86.3±0.3	86.4±0.2	84.9±0.3	63.9±0.3	91.5±0.1	91.7±0.1	91.5±0.1	80±0.4	93.1±0.1	93.1±0.3	92±0.2	83.3±0.3
CLBC												
S_M_C	86.1±0.1	86.4±0.2	85.9±0.3	65.7±0.3	92.4±0.02	92.4±0.2	92.7±0.3	86.2±0.6	92.1±0.1	92.2±0.2	92±0.2	89.4±0.2
CLTC												
S_M_C	89.02±0.06	89.12±0.14	86.42±0.18	67.3±0.40	92.6±0	92.62±0.15	92.46±0.13	86.38±0.26	91.8±0.09	91.86±0.10	92.1±0.11	89.66±0.19
LTP	68.50±0.1	69±0.2	66.50±0.30	39.50±0.50	78.60±0	79.1±0.1	78.90±0.30	60.40±0.60	83.5±0.1	83.6±0.2	82.4±0.4	70±0.4

outperforms over all other LBP variants using CURET database. Table 9 and 10 provides the similar observations on UIUC. It is also noticed that CLTC\_S\_M\_C achieved better results when compared to LBP and LTP and good results when compared to CLBP\_S\_M\_C and CLBC\_S\_M\_C for N = 12, 23 on CURET and N = 10, 15 on UIUC. CLTC\_S\_M\_C has obtained minimum range of variability in classification accuracy which is observed when compared to existing LBP variants on all case studies.

**CONCLUSION**

A texture descriptor plays a significant role in texture classification. Most of the LBP variants are well known methods in characterizing texture of the image. Apart from the successes in various applications, these are suffered from noise sensitivity and rotation variance. This study proposed with dual capability, a rotation invariance and noise insensitivity texture descriptor Completed Local Ternary Count (CLTC) based on ternary count. The performance of CLTC is studied by comparing with various LBP variants using 11 case studies. The experimental results have shown the rotation invariance and increased noise insensitive capability of CLTC with improved classification accuracy over all the other existing LBP variants.

Though the CLTC is more robust to noise when compared to the existing methods, a reduced performance is observed when SNR = 20 dB. This limitation can be

overcome by changing the thresholding process. The computational time of CLTC is more when compared to CLBC. This drawback can be eliminated by reducing the size of feature set. Hence, further research should be directed towards developing a more robust rotation invariant texture descriptor at any SNR with less computation time. This research can be further extended to extract the texture features from color images. These efforts are strongly believed to improve the performance in texture classification and its applications.

**REFERENCES**

Ahonen, T., A. Hadid and M. Pietikainen, 2006. Face description with local binary patterns: Application to face recognition. *IEEE Trans. Pattern Anal. Mach. Intell.*, 28: 2037-2041.

Cao, X.Q., J. Zeng and Z.Q. Liu, 2010. Human body parts tracking using sequential markov random fields. *Proceedings of the 2010 IEEE 20th International Conference on Pattern Recognition (ICPR'10)*, August 23-26, 2010, IEEE, Istanbul, Turkey, ISBN:978-1-4244-7542-1, pp: 1759-1762.

Dan, Z., Y. Chen, Z. Yang and G. Wu, 2014. An improved local binary pattern for texture classification. *Optik Intl. J. Light Electron. Optics*, 125: 6320-6324.

Dana, K.J., B. van Ginneken, S.K. Nayar and J.J. Koenderink, 1999. Reflectance and texture of real-world surfaces. *ACM Trans. Graphics (TOG)*, 18: 1-34.



- Guo, Z., L. Zhang and D. Zhang, 2010a. A completed modeling of local binary pattern operator for texture classification. *IEEE Trans. Image Process.*, 19: 1657-1663.
- Guo, Z., L. Zhang and D. Zhang, 2010b. Rotation invariant texture classification using LBP Variance (LBPV) with global matching. *Pattern Recogn.*, 43: 706-719.
- Hadid, A., J. Ylioinas, M. Bengherabi, M. Ghahramani and A. Taleb-Ahmed, 2015. Gender and texture classification: A comparative analysis using 13 variants of local binary patterns. *Pattern Recognit. Lett.*, 68: 231-238.
- Hafiane, A., K. Palaniappan and G. Seetharaman, 2015. Joint adaptive median binary patterns for texture classification. *Pattern Recognit.*, 48: 2609-2620.
- Hammouche, K., O. Losson and L. Macaire, 2016. Fuzzy aura matrices for texture classification. *Pattern Recognit.*, 53: 212-228.
- Haralick, R.M., K. Shanmugam and I.H. Dinstein, 1973. Textural features for image classification. *IEEE Trans. Syst. Man Cybern.*, SMC-3: 610-621.
- Khellah, F.M., 2011. Texture classification using dominant neighborhood structure. *IEEE. Trans. Image Process.*, 20: 3270-3279.
- Lam, W.K. and C.K. Li, 1997. Rotated texture classification by improved iterative morphological decomposition. *IEE. Proc. Vision Image Signal Process.*, 144: 171-179.
- Lazebnik, S., C. Schmid and J. Ponce, 2005. A sparse texture representation using local affine regions. *IEEE Trans. Pattern Anal. Mach. Intell.*, 27: 1265-1278.
- Liao, S., M.W.K. Law and A.C.S. Chung, 2009. Dominant local binary patterns for texture classification. *IEEE Trans. Pattern Anal. Mach. Intell.*, 18: 1107-1118.
- Nanni, L., A. Lumini and S. Brahmam, 2010. Local binary patterns variants as texture descriptors for medical image analysis. *Artif. Intell. Med.*, 49: 117-125.
- Ojala, T., M. Pietikainen and T. Maenpaa, 2002a. Multiresolution gray-scale and rotation invariant texture classification with local binary patterns. *IEEE Trans. Pattern Anal. Mach. Intell.*, 24: 971-987.
- Ojala, T., T. Maenpaa, M. Pietikainen, J. Viertola and J. Kyllonen *et al.*, 2002b. Outex-new framework for empirical evaluation of texture analysis algorithms. *Proceedings of the 16th International Conference on Pattern Recognition Vol. 1, August 11-15, 2002, IEEE, Quebec, Canada, ISBN:0-7695-1695-X, pp: 701-706.*
- Ouamane, A., M. Belahcene, A. Benakcha, S. Bourenmane and A. Taleb-Ahmed, 2016. Robust multimodal 2D and 3D face authentication using local feature fusion. *Signal, Image Video Process.*, 10: 129-137.
- Ryu, J., S. Hong and H.S. Yang, 2015. Sorted consecutive local binary pattern for texture classification. *IEEE. Trans. Image Process.*, 24: 2254-2265.
- Shrivastava, N. and V. Tyagi, 2014. An effective scheme for image texture classification based on binary local structure pattern. *Visual Comput.*, 30: 1223-1232.
- Song, K., Y. Yan, Y. Zhao and C. Liu, 2015. Adjacent evaluation of local binary pattern for texture classification. *J. Visual Commun. Image Represent.*, 33: 323-339.
- Tan, X. and B. Triggs, 2010. Enhanced local texture feature sets for face recognition under difficult lighting conditions. *IEEE Trans. Image Process.*, 19: 1635-1650.
- Xu, X., J. Li, X. Huang, M.D. Mura and A. Plaza, 2016. Multiple morphological component analysis based decomposition for remote sensing image classification. *IEEE. Trans. Geosci. Remote Sens.*, 54: 3083-3102.
- Zhang, J. and T. Tan, 2002. Brief review of invariant texture analysis methods. *Pattern Recogn.*, 35: 735-747.
- Zhao, G. and M. Pietikainen, 2007. Dynamic texture recognition using local binary patterns with an application to facial expressions. *IEEE Trans. Pattern Anal. Mach. Intell.*, 29: 915-928.
- Zhao, Y., D.S. Huang and W. Jia, 2012. Completed local binary count for rotation invariant texture classification. *IEEE Trans. Image Process.*, 21: 4492-4497.
- Zhao, Y., L. Zhang, P. Li and B. Huang, 2007. Classification of high spatial resolution imagery using improved Gaussian Markov random-field-based texture features. *IEEE. Trans. Geosci. Remote Sens.*, 45: 1458-1468.
- Zhao, Y., W. Jia, R.X. Hu and H. Min, 2013. Completed robust local binary pattern for texture classification. *Neurocomputing*, 106: 68-76.